



Anomalous seismic structure beneath the Klyuchevskoy Group, Kamchatka

Alex Nikulin,¹ Vadim Levin,¹ Ashley Shuler,² and Michael West³

Received 6 May 2010; accepted 19 May 2010; published 29 July 2010.

[1] The Klyuchevskoy Group is among the most active volcanic features on Earth, yet its position within the Kamchatka subduction zone is hard to explain with a simple tectonic mechanism. The geochemistry of Klyuchevskoy Group lavas is typical for volcanic products resulting from flux melting in the mantle wedge, yet the depth to the subducting Pacific plate beneath it is much larger than the average depth of volatile release in subduction zones. We present new seismological constraints on the upper mantle structure beneath the Klyuchevskoy Group and identify a planar dipping seismic feature in the mantle wedge which is ~100 km deep and appears to be sharply bounded. We hypothesize that this upper mantle structure may be the true source of melts erupting at the Klyuchevskoy Group, and that the presence of this feature may explain both the extraordinary productivity of the Klyuchevskoy Group and its unusual location. **Citation:** Nikulin, A., V. Levin, A. Shuler, and M. West (2010), Anomalous seismic structure beneath the Klyuchevskoy Group, Kamchatka, *Geophys. Res. Lett.*, 37, L14311, doi:10.1029/2010GL043904.

1. Introduction

[2] The geographical position of arc volcanoes is controlled by the depth to the subducting plate. In surveys of global seismicity [Syracuse and Abers, 2006; England et al., 2004] the depth to the subducting plate beneath arc volcanoes ranges from 70 to 250 km. Estimates of the global average depth of a subducting plate beneath the arc are close to 110 km, e.g. 108 ± 14 km [Tatsumi and Eggins, 1995]; 112 ± 19 km [Tatsumi, 1986] and 124 ± 38 km [Gill, 1981]. At a depth of ~100 km temperature and pressure conditions favor release of volatiles from the downgoing plate in most subduction zone environments [Davies and Stevenson, 1992].

[3] The Klyuchevskoy Group (KG) in Kamchatka (Figure 1) is composed of active and dormant volcanic centers which, when taken together, comprise the single most active arc volcanic center in the world [Popolitov and Volynets, 1982]. However, estimates of the depth to the subducting slab beneath the KG area are 150–200 km [e.g., Gorbatov et al., 1997; Avdeiko et al., 2007; Portnyagin and Manea, 2008], exceeding the global average.

[4] While the depth to the subducting plate beneath the KG is exceptional, the chemical composition of KG volcanic products is typical of arc volcanoes. Geochemical tracers extracted from KG lavas suggest flux melting under normal arc conditions [Ishikawa et al., 2001]. It is not clear how a large volcanic center with seeming dependence on dehydration-induced melting can sustain its activity in its current position relative to the subducting Pacific plate.

[5] In this paper we describe a newly identified seismic anomaly beneath the KG. Its presence at ~100 km in the upper mantle may help explain both the intense volcanism and geographical location of the KG.

2. Tectonic Summary

[6] Volcanoes of Kamchatka can be grouped into three geographic clusters, each distinct in chemical composition and age (Figure 1). The active Eastern Volcanic Belt (EVB) stretches parallel to the active subduction trench and hosts volcanic complexes ranging from extinct Pliocene to active Holocene volcanoes [Volynets, 1994]. The nearly extinct Sredinny Range (SR) is located to the west of the EVB. The Central Kamchatka Depression (CKD), which separates the EVB and SR, contains volcanic complexes composed of basalts, basaltic andesites and andesites which are Late Pleistocene to Holocene in age [Avdeiko et al., 2007]. Volcanoes of the CKD are geographically offset to the west relative to the EVB (Figure 1), a fact often explained by the shallowing of the subducted slab [Gorbatov et al., 1997; Jiang et al., 2009]. Interestingly, while the shallowing is gradual [Avdeiko et al., 2007] the offset is abrupt, with CKD and EVB volcanoes following the same linear trend.

[7] Lavas of all Kamchatkan volcanoes are enriched in large ion lithophile elements (Rb, Ba, K, Pb, Sr, Li, and B) with respect to high field strength elements (Nb, Zr and Ti) [Ishikawa et al., 2001; Avdeiko et al., 2007], a trend associated with arc volcanism. Observed $\delta^{11}\text{B}$ trends show unusually high values for CKD samples (+1.8–+3.6%), and indicate higher flux input than SR or EVB lavas. This observation is not consistent with the proposed slab depth beneath the CKD [Ishikawa et al., 2001]. A mechanism to hydrate the mantle wedge above a deep subducting slab is uncertain, as previous studies have ruled out hydrated sediment input into the trench [Kersting and Arculus, 1995], forearc hydrous mineral input [Schmidt and Poli, 1998], and unusual thermal conditions of the slab [Tatsumi et al., 1994; Yagodinski et al., 2001].

[8] The crust of the CKD was investigated using active source techniques (summarized by Balesta et al. [1977]) and teleseismic receiver function analysis [Levin et al., 2002]. Crustal thickness estimates are between 30 and 40 km, with active source studies yielding lower values. A pioneering

¹Department of Earth and Planetary Sciences, Rutgers University, Piscataway, New Jersey, USA.

²Lamont-Doherty Earth Observatory, Department of Earth and Environmental Sciences, Earth Institute at Columbia University, Palisades, New York, USA.

³Geophysical Institute, University of Alaska Fairbanks, Fairbanks, Alaska, USA.

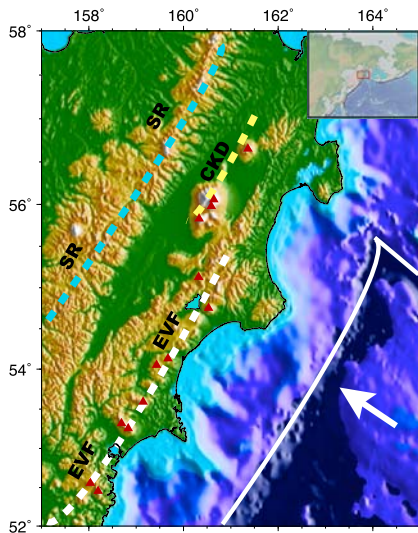


Figure 1. Map of the Kamchatka subduction zone showing major geological and geographical features and the plate motion direction. Dashed lines mark the geographical orientation of volcanic clusters. White arrow represents the direction of subduction and red triangles mark active volcanoes. CKD, Central Kamchatka Depression; EVB, Eastern Volcanic Front; SR, Sredinny Range.

study by *Firstov and Shirokov* [1971] used earthquakes beneath the KG to outline an anomalous feature 80–110 kilometers deep in the upper mantle above the Wadati-Benioff zone. This feature was found to attenuate P and S waves much more than the surrounding mantle. More recent tomographic imaging studies by *Gorbatov et al.* [1999] and *Gontovaya et al.* [2008] that used local earthquake data from much larger networks identified a dipping low-velocity feature in the upper mantle beneath the CKD, ranging in depth from 50 to over 100 km. Studies utilizing teleseismic data [*Lees et al.*, 2007; *Jiang et al.*, 2009] resolve the lateral extent of the Pacific slab and identify slower seismic speed in the wedge above, but cannot constrain details of the wedge structure.

3. Data and Methods

[9] Since 2006 the US-Russian collaborative Partnerships in Research and Education (PIRE) has operated a local broadband seismic network in the KG. We use data from three adjacent PIRE stations recorded in 2006 and 2007. Geographically, the stations form a triangle on the edifice of Bezymianny volcano in the center of the KG (Text S1 of the auxiliary material).¹ The small distance between stations allows us to combine records to increase the signal-to-noise ratio, and thus compensate for the relatively short period of observation time of ~2 years. For this study, we selected earthquakes with magnitude over 5.5 located 20°–90° from the stations. These selection criteria yielded 166 earthquake-station pairs (Figure S3 and Table ST1 of Text S1).

[10] Teleseismic P-waves generate accompanying shear waves as a result of interaction between the primary wave and

encountered material interfaces [*Phinney*, 1964; *Vinnik*, 1977]. Receiver functions (RFs) describe recorded sequences of P-to-S converted wave phases generated at each interface encountered by the primary wave. Receiver-function analysis has been successfully used to detect velocity contrasts associated with subducted slabs [*Langston*, 1981; *Ferris et al.*, 2003; *Park et al.*, 2004; *Nikulin et al.*, 2009]. We use the multitaper correlation (MTC) receiver-function estimator [*Park and Levin*, 2000] to compute frequency domain RFs. We average individual RF estimates weighted by their uncertainties in the frequency domain. We use overlapping 10°-wide bins in back-azimuth and epicentral distance, and present resulting receiver functions in the form of directional or epicentral distance gathers. To aid in the interpretation of RFs we overlay the gathers with graphs of predicted P-to-S delay computed for different positions and orientations (strikes and dips) of velocity interfaces beneath the site. These exact computations assume a plane wave interacting with a single interface beneath the surface (see *Nikulin et al.* [2009] for details).

4. Results

[11] Figure 2 shows a back-azimuth gather of radial RFs computed with an upper frequency limit of 0.375 Hz. Stacked receiver functions show strong coherent positive phases at time delays of ~3.5, ~6 and ~11–13 s (this pulse has a direction-dependent delay). We also see a strong negative phase at ~9–11 s, also with a direction-dependent delay.

[12] To constrain crustal thickness beneath the KG, we calculate delay times for horizontal interfaces at depths of 20, 30 and 40 km, with wave speed changing from 8.0 below to 6.4 km/s above the interface. S wave speed is calculated using a V_p/V_s ratio of 1.75. Large positive pulses at ~3.5 and ~6 s are close to predicted arrivals from horizontal interfaces at ~30 and ~50 km depth. Both converted pulses may represent an upward transition from fast to slow velocities, and thus may be candidates for the crust-mantle boundary. In the epicentral gather (Figure S2 of Text S1), the pulse at ~6 s exhibits the characteristic moveout associated with a multiple reflection. Thus we interpret the ~3.5 s pulse as the crust-mantle interface at ~30 km. This interpretation agrees well with results from deep seismic sounding work [*Balesta et al.*, 1977], and with RFs at a site ~40 km to the south [*Levin et al.*, 2002].

[13] Both the positive pulse at 11–13 s and the preceding negative pulse at 9–11 s follow the same sinusoidal pattern with backazimuth. The pattern is consistent with a dipping interface at depth. The order of pulses (negative earlier than positive) is consistent with conversions from boundaries of a low-velocity layer. We compute P-to-S phase delays for dipping interfaces embedded in the otherwise homogeneous upper mantle wedge with P-wave speed of 8 km/s [*Gorbatov et al.*, 1999; *Gontovaya et al.*, 2008], and $V_p/V_s = 1.75$. We vary the strike and dip of the interface to match the sinusoidal pattern, and vary the depth beneath the station to match the timing. The optimal solution is for an interface 110 km deep dipping 35° to the north (Figure 2).

[14] The pulse sequence remains stable at lower (0.25 Hz) and higher (0.5 Hz) cut-off frequencies, retaining its position in time and the sinusoidal pattern with respect to backazimuth. Assuming that P-to-S converted phases sense wave speed gradients shorter than a quarter of the seismic

¹Auxiliary materials are available in the HTML. doi:10.1029/2010GL043904.

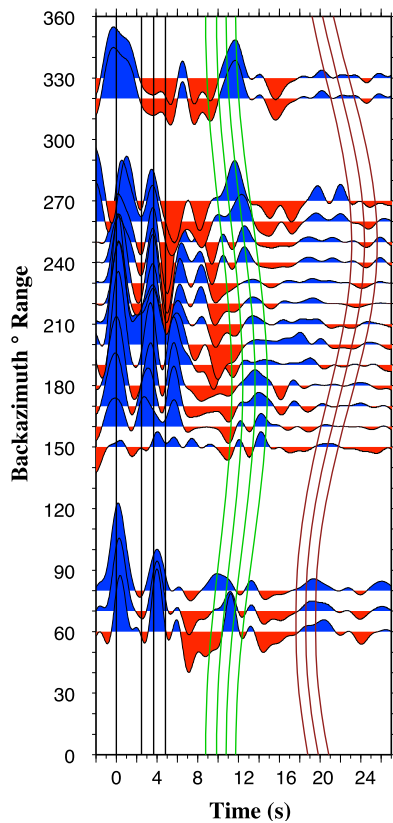


Figure 2. Backazimuthal RF gather and predicted delay times for P-to-S converted phases. Blue lines show expected times for conversions from horizontal interfaces at 30, 40 and 50 km. A positive phase at ~ 3.5 s likely originates at the 30 km deep Moho discontinuity. Green lines show P-to-S converted phases expected from interfaces at 90, 100, 110 and 120 km, dipping 35° to the north. Closely spaced negative and positive pulses between 9 and 13 s follow the predicted pattern, and are matched well by the interface at 110 km. Red lines show expected arrivals from the top of the Pacific slab, represented by interfaces at 180, 190 and 200 km, dipping 35° towards $N310^\circ W$. A relatively weak negative-positive sequence appears to match a pattern for the interface at 190 km.

wavelength as “sharp” [Widess, 1973], shear waves with a period of 2 s traveling in the mantle at 4.6 km/s will be sensitive to changes over ~ 2.25 km. The presence of abrupt seismic wave speed changes over such short distances is not typically expected within the mantle wedge of a subduction zone.

5. Discussion

[15] Imaging interfaces at depths of ~ 100 km using RFs is complicated by interference from Moho multiples. However, a number of pulse characteristics allow us to discriminate between the signals from true structure at this depth and the multiples. The Moho appears to be flat beneath the KG, as indicated by directional stability of the timing of the 3.5 s pulse. In contrast, the 9–13 s pulse arrival time changes systematically with backazimuth. Furthermore, the 9–13 s pulse is two-lobed, with a negative lobe preceding the

positive. This is not consistent with the expected polarities of the Moho multiples, where the earlier lobe should have the same polarity (positive) as the “parent” Moho pulse. Based on these considerations we treat the two-lobed P-to-S converted pulse sequence between 9 and 13 s as arising from a true feature, a low-velocity layer at ~ 100 km depth, inclined $\sim 35^\circ$ to the north.

[16] Figure 3 shows the seismic anomaly with respect to the KG volcanoes and the subducted slab. The area of best RF sampling is to the south-west of Bezymianny volcano. Due to its dip the feature is ~ 80 km deep here, and is clearly separated from the top of the downgoing plate as outlined by local seismicity. Section BB' shows rapidly changing depth to the Pacific slab under CKD volcanoes, from ~ 200 km beneath section AA' to ~ 100 km under Shiveluch volcano. The nearly linear alignment of CKD volcanoes on the map (Figures 1 and 3) conflicts with the concave slab surface outlined by seismicity. If depth to the slab (e.g., of 100 km) controls CKD volcano positions, their locations should form an arcuate trend.

[17] We propose that the low-velocity inclined layer we infer beneath the KG is analogous to the zone of high seismic attenuation and low velocities noted in previous studies [Firstov and Shirokov, 1971; Gorbatov et al., 1997; Gontovaya et al., 2008]. We refer to this feature as the Klyuchevskoy Upper Mantle Anomaly (KUMA) and discuss a number of scenarios that can explain its presence in the upper mantle beneath the KG.

[18] Flow of asthenospheric mantle around the truncated edge of the Pacific slab is suggested by geochemical trends of lavas [Yogodzinski et al., 2001] as well as seismic anisotropy indicators [Peyton et al., 2001]. Such flow can lead to thermal anomalies extending along the strike of the slab, and to a complicated melt generation regime. However, a mechanism of concentrating melts into a planar north-dipping body in the mantle wedge is unclear. Also, while geochemical evidence of slab edge melts is found in Shiveluch lavas [Yogodzinski et al., 2001], it is absent in KG lavas [Portnyagin and Manea, 2008]. Together with weak seismic anisotropy [Peyton et al., 2001], this likely points to weak flow that does not extend to the KG.

[19] Avdeiko et al. [2007] used gravity measurements and tectonic reconstructions to argue for a detached oceanic plate fragment left beneath Kamchatka during the reorganization of the subduction zone geometry ~ 5 Ma ago. Assuming that this fragment had thickened oceanic crust, it would appear as a low velocity layer with a distinct orientation at depth, detectable with RF analysis. Furthermore, if the lithospheric fragment retained some of the volatiles bound in hydrous phases within the crust, their progressive release at ~ 100 km depth would lead to melting in the mantle wedge, and contribute to the eruptive flux of the KG, potentially explaining its elevated level of volcanic activity. However, it remains unclear how a relatively large fragment of oceanic lithosphere could remain suspended in the mantle wedge for a prolonged period of time.

[20] An intriguing explanation of the KUMA is a plume of sediments, either rising from a depth of ~ 200 km [Gerya and Yuen, 2003] or else propagating into the mantle wedge laterally [Currie et al., 2007]. This scenario would explain the low velocities, and a body of sediments will likely form sharp seismic contrasts with wedge material, as observed. It is harder to explain the planar dipping geometry of the feature

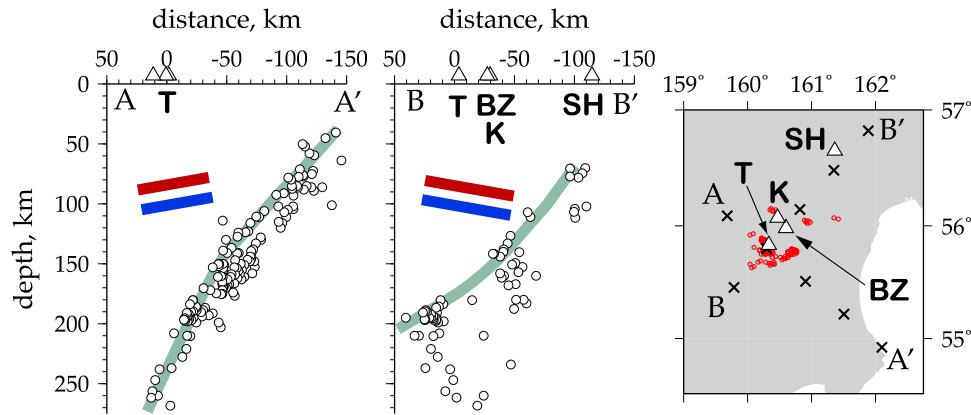


Figure 3. Position of the KUMA (red-blue bar) with respect to the subducting Pacific plate outlined by seismicity and the CKD volcanoes. Vertical cross-sections show earthquakes (circles) located over 10 years (2000–2009) by the Kamchatka Branch of the Geophysical Service of Russian Academy of Sciences. The online catalog (www.emsd.ru) includes events with $M = 3.5$ and larger. Cross-sections are centered on the Tolbachik volcano, aligned along A-A' and normal B-B' to the Pacific plate motion direction, and include events within 25 km of the profile. Crosses on the map correspond to 50 km tick marks on the distance axes of cross-sections, red circles denote 100 km depth pierce points of 166 individual rays from earthquakes used to construct RF gather in Figure 2. CKD volcanoes marked by triangles: BZ, Bezymianny; K, Klyuchevskoy; T, Tolbachik; SH, Shiveluch.

we infer. Simulations by *Currie et al.* [2007] yield cross-sections very similar to AA', but these simulation were only performed in 2D. Also, results of geochemical studies to date did not find a clear signature of sediment-derived melts in the KG lavas [*Kersting and Arculus*, 1995].

[21] Due to the planar geometry of KUMA and its location relatively far from the plate's edge, we do not favor 3D flow around this feature as an explanation for the observed seismic structure. Temperature anomalies alone are unlikely to produce sharp seismic contrasts, and it not clear why excess melt caused by higher temperature would form a layer. Choosing between a suspended cold lithosphere fragment and a propagating cold sediment plume is harder, as we need better images of seismic structure, and additional geochemical constraints.

[22] Regardless of its exact origin, we contend that the KUMA is an important component of the Kamchatka subduction zone. Located at the typical depth of volatile release within the mantle wedge, it is a potential source of melts erupting at the KG. The role of KUMA as a melt generation source must be verified by further studies, but if confirmed its presence may explain the position of the KG relative to the subducting Pacific Plate and its elevated level of volcanic activity.

[23] **Acknowledgments.** Alex Nikulin and Ashley Shuler acknowledge the support and inspiration provided by the PIRE project of the National Science Foundation. The Kamchatka Branch of the Russian Geophysical Service (KBGS) assembled the earthquake catalog. Figures are drafted using the GMT software [*Wessel and Smith*, 1991]. Manuscript benefited from two anonymous reviews and the kind editorial guidance by Ruth Harris. Alex Nikulin acknowledges support from Graduate School of Rutgers University, New Brunswick.

References

Avdeiko, G. P., D. P. Savelyev, A. A. Palueva, and S. V. Popruzhenko (2007), Evolution of the Kurile-Kamchatkan volcanic arcs and dynamics of the Kamchatka-Aleutian Junction, in *Volcanism and Subduction:*

- The Kamchatka Region, Geophys. Monogr. Ser.*, vol. 172, edited by J. Eichelberger et al., pp. 37–55, AGU, Washington, D. C.
- Balesta, S. T., A. I. Farberov, V. S. Smirnov, A. A. Tarakanovsky, and M. I. Zubin (1977), Deep crustal structure of the Kamchatkan volcanic regions, *Bull. Volcanol.*, *40*, 260–266, doi:10.1007/BF02597568.
- Currie, C. A., C. Beaumont, and R. S. Huismans (2007), The fate of subducted sediments: A case for backarc intrusion and underplating, *Geology*, *35*, 1111–1114, doi:10.1130/G24098A.1.
- Davies, J. H., and D. J. Stevenson (1992), Physical model of source region of subduction zone volcanics, *J. Geophys. Res.*, *97*, 2037–2070, doi:10.1029/91JB02571.
- England, P., R. Engdahl, and W. Thatcher (2004), Systematic variation in the depths of slabs beneath arc volcanoes, *Geophys. J. Int.*, *156*, 377–408, doi:10.1111/j.1365-246X.2003.02132.x.
- Ferris, A., G. A. Abers, D. H. Christensen, and E. Veenstra (2003), High resolution image of the subducted Pacific (?) plate beneath central Alaska, 50–150 km depth, *Earth Planet. Sci. Lett.*, *214*, 575–588, doi:10.1016/S0012-821X(03)00403-5.
- Firstov, P. P., and V. A. Shirokov (1971), Seismic investigation of the roots of the Klyuchevskaya group volcanoes, Kamchatka, *Bull. Volcanol.*, *35*, 164–172, doi:10.1007/BF02596814.
- Gerya, T. V., and D. A. Yuen (2003), Rayleigh-Taylor instabilities from hydration and melting propel “cold plumes” at subduction zones, *Earth Planet. Sci. Lett.*, *212*, 47–62, doi:10.1016/S0012-821X(03)00265-6.
- Gill, J. (1981), *Orogenic Andesites and Plate Tectonics*, Springer, New York.
- Gontovaya, L. I., S. V. Popruzhenko, I. V. Nizkous, and S. E. Aprelkov (2008), Upper mantle beneath Kamchatka and its relation to tectonics, *Russ. J. Pac. Geol.*, *2*, 165–174, doi:10.1134/S1819714008020073.
- Gorbatov, A., V. Kostoglodov, S. Gerardo, and E. Gordeev (1997), Seismicity and structure of the Kamchatka subduction zone, *J. Geophys. Res.*, *102*, 17,883–17,898, doi:10.1029/96JB03491.
- Gorbatov, A., J. Domínguez, G. Suárez, V. Kostoglodov, D. Zhao, and E. Gordeev (1999), Tomographic imaging of the P-wave velocity structure beneath the Kamchatka peninsula, *Geophys. J. Int.*, *137*, 269–279, doi:10.1046/j.1365-246X.1999.00801.x.
- Ishikawa, T., F. Tera, and T. Nakazawa (2001), Boron Isotope and trace element systematics of the three volcanic zones in the Kamchatka arc, *Geochim. Cosmochim. Acta*, *65*, 4523–4537, doi:10.1016/S0016-7037(01)00765-7.
- Jiang, G., D. Zhao, and G. Zhang (2009), Seismic tomography of the Pacific slab edge under Kamchatka, *Tectonophysics*, *465*, 190–203, doi:10.1016/j.tecto.2008.11.019.
- Kersting, A. B., and R. J. Arculus (1995), Pb isotope composition of Klyuchevskoy volcano, Kamchatka and north Pacific sediments: Implications for magma genesis and crustal recycling in the Kamchatkan arc, *Earth Planet. Sci. Lett.*, *136*, 133–148, doi:10.1016/0012-821X(95)00196-J.

- Langston, C. A. (1981), Evidence for the subducting lithosphere under southern Vancouver Island and western Oregon from teleseismic P-Wave conversions, *J. Geophys. Res.*, *86*, 3857–3866, doi:10.1029/JB086iB05p03857.
- Lees, J. M., J. VanDecar, E. Gordeev, A. Ozerov, M. Brandon, J. Park, and V. Levin (2007), Three dimensional images of the Kamchatka-Pacific plate cusp, in *Volcanism and Subduction: The Kamchatka Region*, *Geophys. Monogr. Ser.*, vol. 172, edited by J. Eichelberger et al., pp. 293–302, AGU, Washington, D. C.
- Levin, V., J. Park, M. Brandon, J. Lees, V. Peyton, E. Gordeev, and A. Ozerov (2002), Crust and upper mantle of Kamchatka from teleseismic receiver functions, *Tectonophysics*, *358*, 233–265, doi:10.1016/S0040-1951(02)00426-2.
- Nikulin, A., V. Levin, and J. Park (2009), Receiver function study of the Cascadia megathrust: Evidence for localized serpentinization, *Geochem. Geophys. Geosyst.*, *10*, Q07004, doi:10.1029/2009GC002376.
- Park, J., and V. Levin (2000), Receiver functions from multiple-taper spectral correlation estimates, *Bull. Seismol. Soc. Am.*, *90*, 1507–1520, doi:10.1785/0119990122.
- Park, J., H. Yuan, and V. Levin (2004), Subduction-zone anisotropy under Corvallis, Oregon: A serpentinite skidmark of trench-parallel terrane migration?, *J. Geophys. Res.*, *109*, B10306, doi:10.1029/2003JB002718.
- Peyton, V., V. Levin, J. Park, M. Brandon, J. Lees, E. Gordeev, and A. Ozerov (2001), Mantle flow at a slab edge: Seismic anisotropy in the Kamchatka region, *Geophys. Res. Lett.*, *28*, 379–382, doi:10.1029/2000GL012200.
- Phinney, R. A. (1964), Structure of the Earth's crust from spectral behavior of long-period body waves, *J. Geophys. Res.*, *69*, 2997–3017, doi:10.1029/JZ069i014p02997.
- Popolitov, E. I., and O. N. Volynets (1982), Geochemistry of Quaternary volcanic rocks from the Kurile-Kamchatka Island arc, *J. Volcanol. Geotherm. Res.*, *12*, 299–316, doi:10.1016/0377-0273(82)90031-2.
- Portnyagin, M., and V. C. Manea (2008), Mantle temperature control on composition of arc magmas along the Central Kamchatka Depression, *Geology*, *36*(7), 519–522, doi:10.1130/G24636A.1.
- Schmidt, M. W., and S. Poli (1998), Experimentally based water budgets for dehydrating slabs and consequences for arc magma generation, *Earth Planet. Sci. Lett.*, *163*, 361–379, doi:10.1016/S0012-821X(98)00142-3.
- Syracuse, E. M., and G. A. Abers (2006), Global compilation of variations in slab depth beneath arc volcanoes and implications, *Geochem. Geophys. Geosyst.*, *7*, Q05017, doi:10.1029/2005GC001045.
- Tatsumi, Y. (1986), Formation of the volcanic front in subduction zones, *Geophys. Res. Lett.*, *13*, 717–720, doi:10.1029/GL013i008p00717.
- Tatsumi, W., and S. Eggins (1995), *Subduction Zone Magmatism*, Blackwell Sci., Malden, Mass.
- Tatsumi, Y., Y. Furukawa, T. Kogiso, Y. Yamada, T. Yokoyama, and S. A. Fedotov (1994), A third volcanic chain in Kamchatka: Thermal anomaly at transform/convergence plate boundary, *Geophys. Res. Lett.*, *21*, 537–540, doi:10.1029/94GL00214.
- Vinnik, L. P. (1977), Detection of waves converted from P to SV in the mantle, *Phys. Earth Planet. Inter.*, *15*, 39–45, doi:10.1016/0031-9201(77)90008-5.
- Volynets, O. N. (1994), Geochemical types, petrology and genesis of Late Cenozoic volcanic rocks from the Kurile-Kamchatka island-arc system, *Int. Geol. Rev.*, *36*, 373–405, doi:10.1080/00206819409465467.
- Wessel, P., and W. H. F. Smith (1991), Free software helps map and display data, *Eos Trans. AGU*, *72*, 441, doi:10.1029/90EO00319.
- Widess, M. (1973), How thin is a thin bed?, *Geophysics*, *38*, 1176–1180, doi:10.1190/1.1440403.
- Yogodzinski, G. M., J. M. Lees, T. G. Churikova, F. Dorendorf, G. Woerner, and O. N. Volynets (2001), Geochemical evidence for the melting of subducting oceanic lithosphere at plate edges, *Nature*, *409*, 500–504, doi:10.1038/35054039.

V. Levin and A. Nikulin, Department of Earth and Planetary Sciences, Rutgers University, 610 Taylor Rd., Piscataway, NJ 08854, USA. (alnikulin@gmail.com)

A. Shuler, Lamont-Doherty Earth Observatory, Department of Earth and Environmental Sciences, Earth Institute at Columbia University, 61 Rte. 9W, Palisades, NY 10964, USA.

M. West, Geophysical Institute, University of Alaska Fairbanks, 903 Koyukuk Dr., Fairbanks, AK 99775, USA.